## Risley Prism Scanner

Two wedge prisms can be used to create an angular deviation of a beam from its optical axis to create continuous circular scan patterns or discrete beam pointing, which is commonly referred to as a Risley Prism Scanner. In this App Note, we discuss the principles of a Risley Prism Scanner and demonstrate the development of one such scanner using Thorlabs' components.

# Table of Contents

# Part 1. Single Wedge Prisms and Snell's Law

A Risley Prism Scanner utilizes two wedge prisms to steer a beam. A wedge prism can be thought of as an optical window with one side ground and polished at an angle in order to refract, or bend, the input light. This Application Note will focus on round wedged prisms; these are effectively cylinders with one surface perpendicular to its curved side that will be referred to as the flat face, and a surface opposite of the flat face that will be referred to as the wedged face. Figure 1 shows the cross section of a round wedged prism where the wedged face was ground with a physical angle, $\alpha$, with respect to the flat surface.

Snell's Law, shown in Eq. (1), can be used to determine the angle that the prism refracts the light at each surface. This is done by establishing a relationship between the refractive index of each medium the light will travel through, n, and the angle that the beam creates on either side of the interface with respect to the normal of the interface.

$$n_1 * \sin(\phi_1) = n_2 * \sin(\phi_2) \tag{1}$$
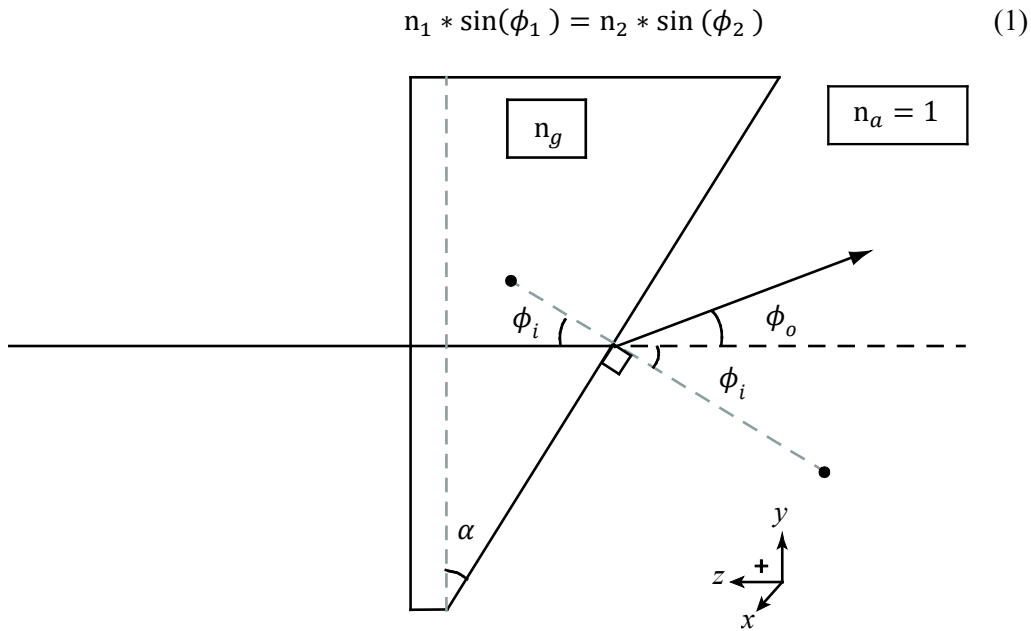


**Figure 1: A beam entering a wedged prism from its flat face and refracting as it hits the wedged face according to Snell's Law. Diagram is not to scale.**

In Figure 1, a monochromatic beam enters through a wedged prism normal to its flat face; this will cause no beam deviation. However, at the wedged face, the beam is incident at $\phi_i$ and refracts with an output angle from its original optical path, $\phi_o$. The refractive index of the glass has been denoted by $n_g$, and it will be assumed here and throughout this App Note that air's index of refraction, $n_a$, is equal to 1.00 and $n_g > n_a$. It is important to emphasize that in this example $n_g > n_a$, so that the beam refracts away from the normal when exiting the prism.

Figure 1 shows the output angle with respect to the original optical axis, but Snell's Law measures refraction angles relative to the normal of the interface. As seen in Figure 1, $\phi_2 = \phi_i + \phi_o$, and Eq. 1 becomes

$$n_g * \sin(\phi_i) = \sin(\phi_i + \phi_o). \tag{2}$$

In Figure 1, the angle of incidence is equal to the physical angle of the prism,[1]

$$\phi_i = \alpha, \tag{3}$$

and solving for the exiting beam angle relative to the input angle provides

$$\phi_o = \sin^{-1}(n_g \sin(\phi_i)) - \phi_i. \tag{4}$$

The physical prism angle will most likely be less than 17°, so the small angle approximation[2] can be applied to Eqs. (4) and (2), which yields

$$\phi_o \approx (n_g - 1)\phi_i \tag{5}$$

as a model of the output angle from the prism. Under the small angle approximation, it can also be shown that the beam can enter from either the flat or wedged side of the prism, and the light will have the same exit angle provided by Eq. (5). [3]

It is important to note that Figure 1 was drawn with the input beam entering the prism at the flat face to provide an example with a single refraction angle. For the all subsequent examples in this App Note the light will enter the first prism at its wedged face.

---

[1] Prisms not aligned with the input beam will be explored in Part 4. Physical Systems and Error.
[2] $\sin(\theta) \approx \sin^{-1}(\theta) \approx \theta$, if $\theta < 0.3$ rad
[3] See Part 7.1. Proof: Small Angle Equation Showing Beam Can Enter from Either Side of a Prism.

## Part 2. Creating a Circular Scan with One Prism

As mentioned at the end of the previous section, consider now a beam entering the wedged side of the prism, as shown in Figure 2. A circular beam path can be formed by rotating this prism. To see how, consider the first interaction upon the prism. This interaction refracts the light within the prism at an angle, $\phi_p$, calculated by Snell's Law, which gives

$$\phi_p = \sin^{-1}\left[\frac{\sin(\phi_i)}{n_g}\right] \approx \frac{\phi_i}{n_g}. \tag{6}$$

To determine the lateral distance the light will travel away from the original optical axis within the thickness of the prism, $r_T$, a right triangle can be created using the thickness of the middle of the prism[4], $T$, and the angle $(\phi_i - \phi_p)$. This distance is

$$r_T = T * \tan(\phi_i - \phi_p). \tag{7}$$

After traveling the thickness of the prism, the beam becomes incident on the flat face. Using the output angle found in Eq. (5) and the distance along the original optical axis between the flat face of the prism and an observation screen or sensor, S, the lateral displacement of the beam can be calculated as

$$r_S = S * \tan(\phi_o). \tag{8}$$

The total lateral deviation of the exit beam, $r'$, from the original optical axis at the observation screen when entering from the wedged side becomes

$$r' = r_S + r_T = S * \tan(\phi_o) + T * \tan(\phi_i - \phi_p). \tag{9}$$

---

[4] $T = \left(T_{max} - \frac{1}{2} * \mathcal{D} * \tan(\alpha)\right)$, where $T_{max}$ is the thickest section of the prism and $\mathcal{D}$ is the prism's diameter.
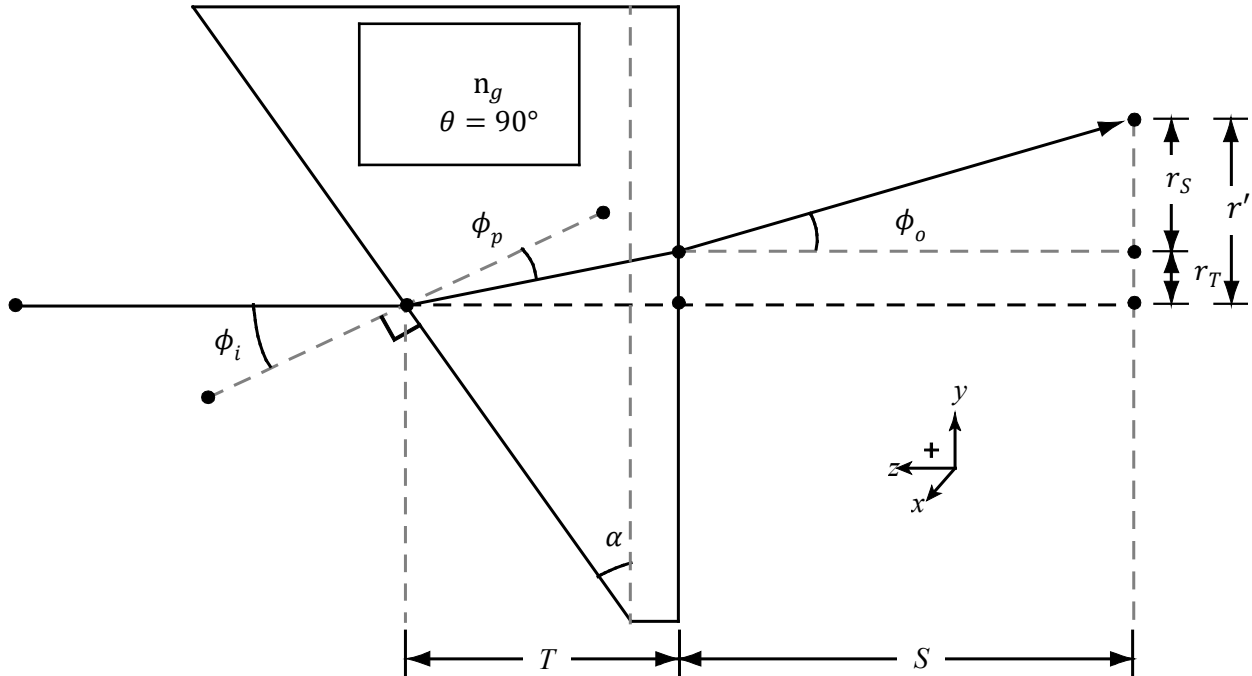
**Figure 2: The beam path of a monochromatic source incident on the wedged side of a round wedged prism, which has its thickest section defined as vertical. Diagram is not to scale.**

As the title of this subsection indicates, this setup should be able to scan or point the output beam in a two dimensional, circular pattern on the observation screen. In Figures 1 and 2, the orientation of the prism was always shown with the thickest part of the prism at the top of the diagram. If the prism was rotated about the original optical axis with angle $\theta$ in the xy-plane, the beam would trace out a circle with a radius of $r'$, found in Eq. (9). For the purpose of this App Note, the home position, $\theta = 90°$, will be defined as when the thickest part of the prism is aligned to the top of the page. Assuming the rotation direction is positive when the prism rotates clockwise when looking in the direction of propagation, the position of the output beam on the observation screen for a single prism can be determined using the parametric equations:

$$y(\theta) = r' * \sin(\theta); \quad x(\theta) = r' * \cos(\theta) \tag{10}$$

The rotational position can change through time, $t$, which is defined as angular velocity,

$$\omega = \frac{\theta}{t} \Rightarrow \theta = \omega t. \tag{11}$$

The angular velocity can then be substituted into Eq. (10) to form a time-dependent parametric equation for the position of the beam,

$$y(t) = r' * \sin(\omega t), x(t) = r' * \cos(\omega t). \tag{12}$$

Assuming $\omega$, the angular velocity, and $r'$ are constant, Eq. (12) is the time-dependent parametric equation for a circle. No matter what the prism's rotational speed, the resulting beam path will always form a circle pattern.

Example:

A PS812-A Round Wedge Prism is mounted in a PRM1Z8 Motorized Precision Rotation Mount, with the flat face of the mounted prism 300 mm from a screen. If a 600 nm laser was shot through the center of the prism rotating in the mount at an angular velocity of 10 degrees per second, what are the circle's dimensions when projected onto the viewing screen?

The PS812-A is a 1 inch optic, 8.11 mm at its thickest and with a wedge angle of 11.367°, so the distance a beam would travel through the prism is $T = 8.11 - \frac{[25.4*\tan{(11.367)}]}{2} = 5.557$ mm. At 600 nm, the prism made from NBK- 7 has a refractive index of 1.516.

These values will yield the following:

| | | | |
|---|---|---|---|
| $\phi_i$ | 0.198 rad | $r_T$ | 0.381 mm |
| $\phi_p$ | 0.130 rad | $r_S$ | 31.091 mm |
| $\phi_o$ | 0.103 rad | $r'$ | 31.472 mm |

So, this setup will yield a circular pattern that has a radius of about 31.5mm.

# Part 3. Risley Prism Scanners

## 3.1. Largest and Smallest Scan Area

Two prisms used to refract the same beam can point a beam anywhere in the area of an annulus, or the shape created by two concentric circles. To find the inner and outer bounds of this annulus, a setup is created where two prisms are aligned in succession with the flat faces towards each other [5] and set at the home position, $\theta_1 = \theta_2 = 90°$, as seen in Figure 3. This creates a beam path propagating at twice the exit angle of one prism with respect to the original optical axis.[6] The displacement from the optical axis caused by this final refraction interface can be calculated as

$$r_r = z * \tan(2\phi_o). \tag{13}$$

To split $r_r$ into two parts, each of which are contributions from the individual prisms, a small angle approximation can be applied as [7]

$$r_r \approx 2z * \tan(\phi_o). \tag{14}$$

It can be imagined that the first prism creates a radius, $r_1$, that defines the start of a second, equivalent radius, $r_2$, created by prism 2:

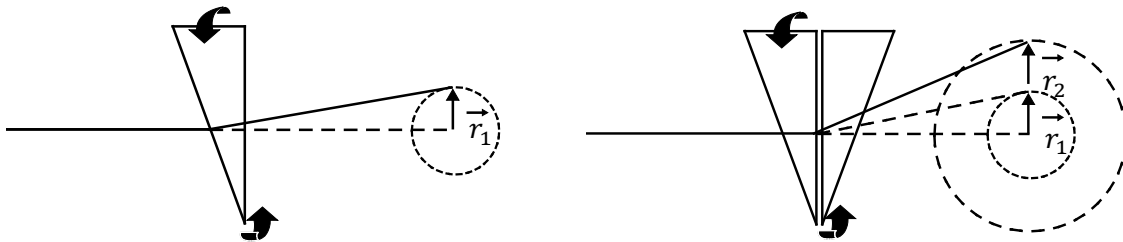$$r_r = r_1 + r_2 \approx z * \tan(\phi_o) + z * \tan(\phi_o) \tag{15}$$



**Figure 3: A visualization of how each prism adds to the maximum beam displacement in a Risley Prism Scanner.**

This exiting beam has also been offset from the original optical path, which will be defined as $r_d$, by the path it took through and between both prisms up to the second surface of the second prism. The distance traveled through the first prism, as shown previously in Figure 2, is $T$. However, the distance traveled through the second prism will change depending on two conditions: $r'$, the lateral displacement caused

---

[5] The orientation of the prisms with flat faces towards or away from each other only marginally changes performance. Flat faces towards each other is preferred as they can be placed as closely together as possible.
[6] See Part 7.2. Proof: Two Prisms Cause Twice the Exit Angle of a Single Prism
[7] See Part 7.4. Inherent Edge Distortion

between the two prisms, and $|\theta_1 - \theta_2|$, the difference in rotation position of the prisms. Noting that $\phi_i = \alpha$, the contribution, $T'$, that is added or taken away from the thickness of the second prism is

$$T' = r' * \tan(\phi_i) * \cos(|\theta_1 - \theta_2|.). \tag{16}$$

The resulting equation becomes

$$r_d = [2T + T'] * \tan(\phi_i - \phi_p) + S * \tan(\phi_o). \tag{17}$$

When $\theta_1 = \theta_2 = 90°$, the point furthest from the origin can be calculated as

$$r_{max} = r_r + r_d \approx [2T + T'] * \tan(\phi_i - \phi_p) + (2z + S) * \tan(\phi_o). \tag{18}$$

Eq. (18) defines the largest distance a deflected beam can point from the original optical axis when traveling through two wedged prisms.
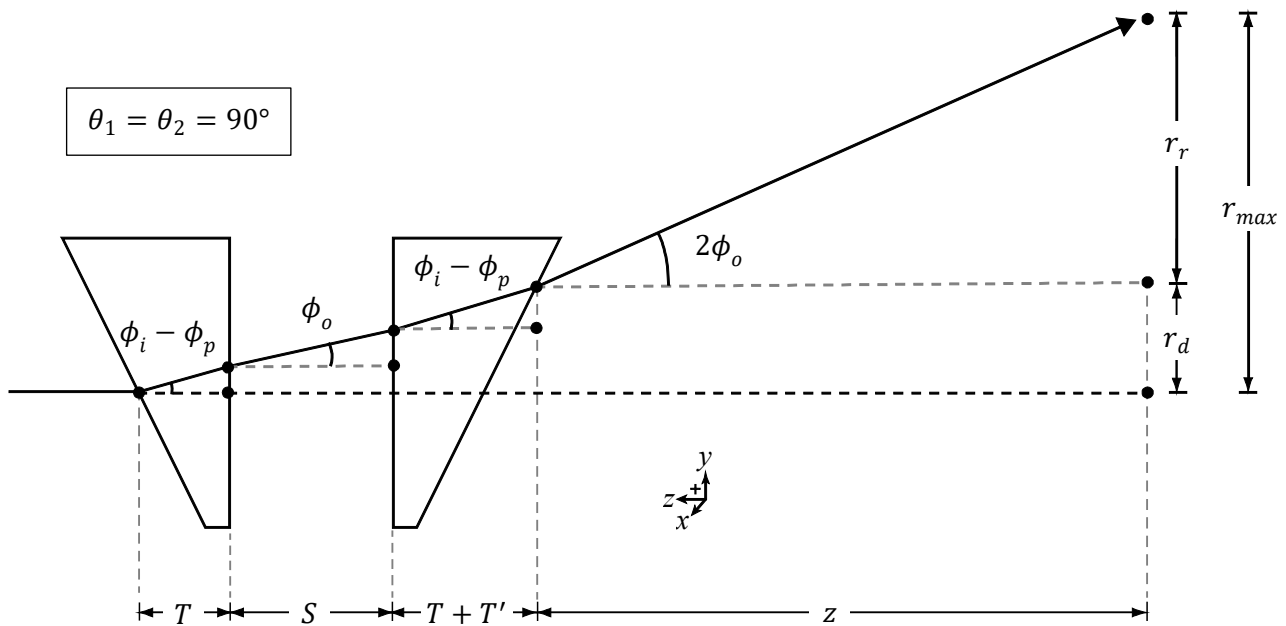


**Figure 4: The beam path taken through a Risley Prism Scanner when both prisms are in the home position, giving the maximum displacement of the beam. Diagram is not to scale.**

If the prisms are aligned in such a way that they have their thickest sides opposite to each other, such that $\theta_1 = 90°$ and $\theta_2 = 270°$, one may assume that the beam would travel straight through the pair without any refraction, as the wedge angles are opposite each other. This is not entirely true. As seen in Figure 5, the contributions from all interfaces cause the beam to remain parallel to the original beam path but be offset by some distance $r_d$. Since the beam is parallel to the original beam path and the refraction

angles induced by the prisms will only increase the output angle, the beam cannot point within $r_d$. For the purposes of this App Note, the area encompassed by $r_d$ will be defined as the center defect.
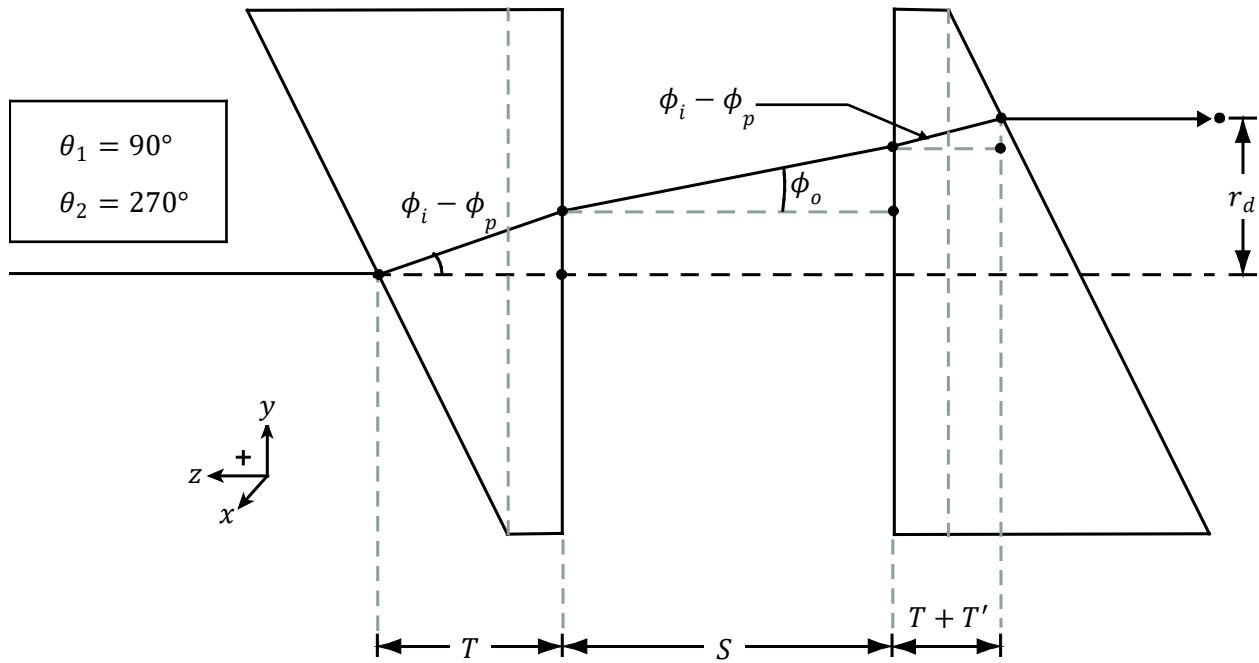


**Figure 5: The beam path taken through a Risley Prism Scanner when the prisms are offset by 180°, giving the smallest scan radius. This radius is caused purely by the beam traveling through the thickness of the prisms and the space between them. Diagram is not to scale.**

If the second prism rotates 360° while the first remains at $\theta = 90°$, the beam traces a circle of radius $r_1$ with a center point $r_2$ from the origin point. The changes each prism makes to the beam path are additive. This means to make a set of equations that will describe this system, a sum of the radii must be created, each dependent on the contribution from each prism

$$y(\theta_1, \theta_2) = r_1 * \sin(\theta_1) + r_2 * \sin(\theta_2) + r_d * \sin(\theta_1),$$
$$x(\theta_1, \theta_2) = r_1 * \cos(\theta_1) + r_2 * \cos(\theta_2) + r_d * \cos(\theta_1), \qquad (19)$$

that can be simplified to,

$$y(\theta_1, \theta_2) = (r_1 + r_d) * \sin(\theta_1) + r_2 * \sin(\theta_2),$$
$$x(\theta_1, \theta_2) = (r_1 + r_d) * \cos(\theta_1) + r_2 * \cos(\theta_2). \qquad (20)$$

Eq. (20) can point the output beam anywhere between the annulus created by $r_{max}$, which defines the system's outer scanning radius, and $r_d$, the area, which the beam cannot hit, called the center defect.

## 3.2. Scans with Constant Rotation Speeds: Rose Curves

Patterns that repeat regularly can be created by a Risley Prism Scanner. To see this, Eq. (11) can be used to augment Eq. (20) to create the following time-dependent parametric equation:

$$y(\omega_1, \omega_2) = (r_1 + r_d) * \sin(\omega_1 t) + r_2 * \sin(\omega_2 t),$$
$$x(\omega_1, \omega_2) = (r_1 + r_d) * \cos(\omega_1 t) + r_2 * \cos(\omega_2 t) \qquad (21)$$

This equation describe a class of shapes called Epitrochoids [ep-i-**troh**-koids].[8] Regular, repeating shapes will be created only when rational values of $\omega_1$ and $\omega_2$ are used to spin the prisms. To create a catalog of regular shapes that can be created by a Risley Prism Scanner, assume $r_1 = r_2 = 1$ and $r_d = 0$.



**Figure 6: A Limaçon formed when** $\frac{\omega_1}{\omega_2} = 2$.

Lines and circles are special cases of Epitrochoids that can be traced with a Risley Prism Scanner. To trace a line, the prisms are spun at the same speed in the opposite direction starting at $\theta_1 = \theta_2 = 90°$; by doing this, the horizontal contributions from each prism are canceled out, leaving only the vertical contributions. To trace the largest possible circle with the Risley Prism Scanner, spin both prisms at the same speed in the same direction.

If both prisms spin in the same direction, with one spinning at twice the speed of the other, the scanner will form a Limaçon, as seen in Figure 6. Trifoliums[9] can be formed if on prism is moving at twice the speed of the other, in the opposite direction as seen in Figure 7.



**Figure 7: A Trifolium formed when** $\frac{\omega_1}{\omega_2} = -2$.

The full family of curves that will repeat regularly are called Rose Curves. A list of some of the possible curves and the relative speeds of the prisms in a Risley Scanner needed to form them can be found in 7.8. If one would want to scan the entire scan area formed between $r_{max}$ and $r_d$, irrational ratios of prism speeds will fill the circular scan area as $t \to \infty$, for example: $\frac{\omega_1}{\omega_2} = \sqrt{2}$, which is shown in Figure 8.
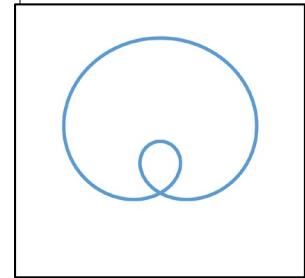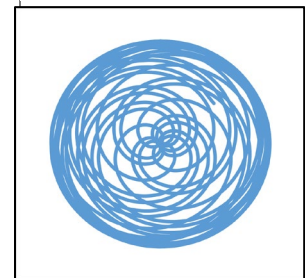


**Figure 8: A space-filling curve with** $\omega_1 = 10\sqrt{2}$ **rps and** $\omega_2 = 10$ **rps over 720 s.**

---

[8] See Part 7.3. Proof: Epitrochoid Equivalence
[9] This curve has many names, including the Three Pedaled Rose and the Paquerette de Mélibée. A variant of this shape is also used as the symbol for Adobe System's Acrobat Software.

# Part 4. Physical Systems and Assembly Error

## 4.1. Home Position Misalignment

Thus far, this App Note has described a perfectly aligned Risley Prism Scanner, but in practice, tolerance stack-up and interfacing will result in a variety of misalignments. Misalignments in the Risley Prism Scanner manifest themselves in different ways. The first to consider is home position misalignment, where one of the prisms does not have its thickest section at the top of its rotation. This can be compensated for by adding a term $\Delta\theta$ to the stationary equation:

$$y(\theta_1, \theta_2) = (r_1 + r_d) * \sin(\theta_1) + r_2 * \sin(\theta_2 + \Delta\theta),$$
$$x(\theta_1, \theta_2) = (r_1 + r_d) * \cos(\theta_1) + r_2 * \cos(\theta_2 + \Delta\theta) \qquad (22)$$

$\Delta\theta$ is the angle difference between the defined and the actual home position. Consequences of home position misalignment existing in a system are explored in Section 7.5.

## 4.2. Prism Tilt in Mount

The model then needs to account for prism tilt, $\beta$, or the angle created when the prisms' flat faces are not perpendicular to the optical axis; this can be caused by retaining rings and spacers not fitting correctly against the prism in a setup. This complication means that each prism will have its own set of values. In the following equations, a subscript of 1 or 2 denotes that the variable relates to the first or second prism in line, respectively. For example, $\phi_{i,2}$ is the angle of incidence upon the second prism. The prism tilt term can be factored into Eq. (3), creating the following incidence angles for both prisms:

$$\phi_{i,1} = \alpha_1 - \beta_1$$
$$\phi_{i,2} = \beta_2 - \phi_{o,1} \tag{23}$$

However, it may be inaccurate to assume that this new incidence angle including the prism tilt is still within the small angle approximation, so the radii terms expressed in Eqs. 4 and 6 should be expanded to:

$$\phi_{o,1} = \sin^{-1}\left[n_{g,1} * \sin\left(\alpha_1 - \sin^{-1}\left(\frac{\sin(\phi_{i,1})}{n_{g,1}}\right)\right)\right] - \beta_1$$

$$\phi_{p,1} = \sin^{-1}\left[\frac{\sin(\phi_{i,1})}{n_{g,1}}\right]$$

$$\phi_{o,2} = \sin^{-1}\left[n_{g,2} * \sin\left(\alpha_2 - \sin^{-1}\left(\frac{\sin(\phi_{i,2})}{n_{g,2}}\right)\right)\right] - \alpha_2 + \beta_1$$

$$\phi_{p,2} = \sin^{-1}\left[\frac{\sin(\phi_{i,2})}{n_{g,2}}\right]$$

With these values, $r_1$, $r_2$, and $r_d$ can be redefined in order to account for prism tilt in the system. A useful consequence of breaking things up this way is that the equations can now also account for two prisms with different prism angles.

$$r' = S * \tan\left(\phi_{o,1}\right) + T_1 * \tan\left(\phi_{i,1} - \phi_{p,1}\right)$$

$$r_d = r' + T_2 * \tan\left(\phi_{i,2} - \phi_{p,2}\right)$$

$$r_1 = z * \tan\left(\phi_{o,1}\right)$$

$$r_2 \approx z * \tan\left(\phi_{o,2}\right)$$

The consequences of prism tilt in a system are explored in Section 7.6. The tilt also has an effect on the size of the center defect, which is explored in Section 7.7.

## *4.3.  Pointing a Beam Discretely*

Rose Curves may be useful depending on the application, but other applications require discrete pointing or a non-continuous beam path, which cannot be created by prisms spinning at a constant speed. For these cases, it is useful to have a function of $\theta(x, y)$. That is to say, what angle each prism needs to be rotated to for a beam to be pointed at certain Cartesian Coordinates (x,y) within the scan area. This can be found[10] by rearranging Eq. (22) to solve for $\theta_1$ and $\theta_2$, which yields

$$\theta_1(x, y) = \cos^{-1}\left(\frac{x^2+y^2+(r_1+r_d)^2-r_2{}^2}{2(r_1+r_d)\sqrt{x^2+y^2}}\right) + \tan^{-1}\left(\frac{y}{x}\right)$$
$$\theta_2(x, y) = \cos^{-1}\left(\frac{x^2+y^2-(r_1+r_d)^2+r_2{}^2}{2r_2\sqrt{x^2+y^2}}\right) + \tan^{-1}\left(\frac{y}{x}\right) - \Delta\theta \tag{24}$$

Using Eq (24), each prism can be rotated as quickly as possible to the desired location to sample a point, within the physical limits of the system. This approach can be used to create raster scans, scans which are made of multiple discrete points, instead of a constant beam path. Eq. (24) will be integrated into a LabVIEW program in the next section to run the Risley Prism Scanner built for this App Note.

---

[10] See Part 7.9. Derivation: Prism Angles as Functions of Scan Pattern Coordinates

# Part 5.  Risley Prism Scanner Test and Analysis

This section describes how a Risley Prism Scanner was created using Thorlabs components, and how it performed. The setup is shown in Figure 9. The prism scanner was controlled with an application-specific LabVIEW program that handled the prims' rotation, the laser's power, and the beam profiler's recording process.

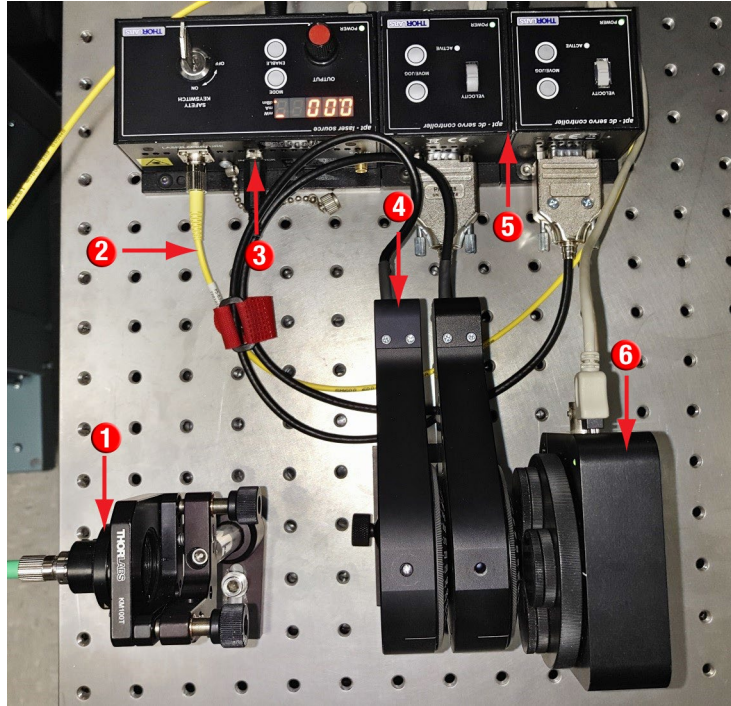## 5.1.  Parts Used to Build the Risley Prism Scanner



**Figure 9: A photo of the Risley Prism Scanner built from Thorlabs components for this App Note.**

1.    A Fiber collimator (TC12FC-633) mounted in a kinematic mount (KM100T). The output laser beam was adjusted to propagate parallel to the optical table along the optical table's screw holes.

2.    A PC/APC single mode fiber (P5-630A-PCAPC-1).

3.    A 635 nm laser source (TLS001-635).

4.    Two wedged prisms (PS810-A) mounted in individual motorized rotation stages (PRM1Z8) using wedged prism mounting shims (SM1W353).

5.    Two DC servo motor controllers (TDC001)

6.    A CCD beam profiler (BS106-VIS).

## *5.2. Initial Alignment*

Careful alignment of the two wedged prisms is critical in order to create the intended scan patterns. To align, follow these steps:

1. Set up an observation screen as far as possible from the setup; a longer distance helps achieve better accuracy of the prism locations. Mark the location of the beam without any prisms in the path as $O_1$. This mark corresponds to the center of the field of view.

2. Insert only the second prism in the laser path with the wedged surface facing the screen, and align the prism such that the reflection from the flat surface travels back into the fiber collimator to make the prism as perpendicular to the original optical axis as possible.

3. Rotate the second prism until the beam reaches the highest position on the observation screen. Record the rotation stage location as the home location for the second prism.

4. Place the first prism into the laser path with the flat side facing the second prism, positioning it as close to the second prism as possible. To make the first prism's flat face perpendicular to the original optical axis, rotate the first prism about the optical axis until the beam output from the second prism is as close to the center of the prism as possible, and then adjust the tilt of the first prism until the beam points to the center of the field of view on the observation screen. Recall, the beam will never hit the center of the field of view due to the center defect.

5. Once aligned, rotate the first prism using the software until the laser reaches the highest position on observation screen. Record the rotation stage location as the home location for the first prism.

6. After the home positions are set, rotate the prisms at the same speed in opposite directions in order to scan a straight line. Measure the angle of the line with respect to a vertical line on the observation screen and record $\Delta\theta$ as half the measured angle.

7. The tilt angles $\beta_1$ and $\beta_2$ can be calculated as follows:

   For $\beta_2$: Rotate the second prism 360°, tracing the resulting circle; mark the position on the circle furthest from $O_1$, labeling it $O_2$. Measure the distance between the two points. $\beta_2$ can be calculated

$$\beta_2 = \tan^{-1}\left(\frac{O_2 - O_1}{z}\right).$$

   For $\beta_1$: First, rotate second prism to put the laser spot at the highest position after $\beta_2$ is calculated. Secondly, insert first prism into system and align the prism. Once aligned, insert a viewing board with a hole between the laser source and the first prism with distance as $d_2$ between the prism and

the board. The hole should let laser pass through. Rotate first prism and record the circle that is made by the reflected beam off of the first prism's wedged surface, and measure the circle diameter D. $\beta_1$ can now be calculated:

$$\beta_1 = \tan^{-1}\left[\frac{D}{2(z+S)}\right] - \alpha_1.$$

## 5.3. Continuous Scans

As stated in Part 3, there are a large variety of patterns that can be generated by controlling the rotation speed and rotation direction of the two wedged prisms. Figure 10 shows patterns generated with the dual wedge scanner that were measure with a beam profiler.
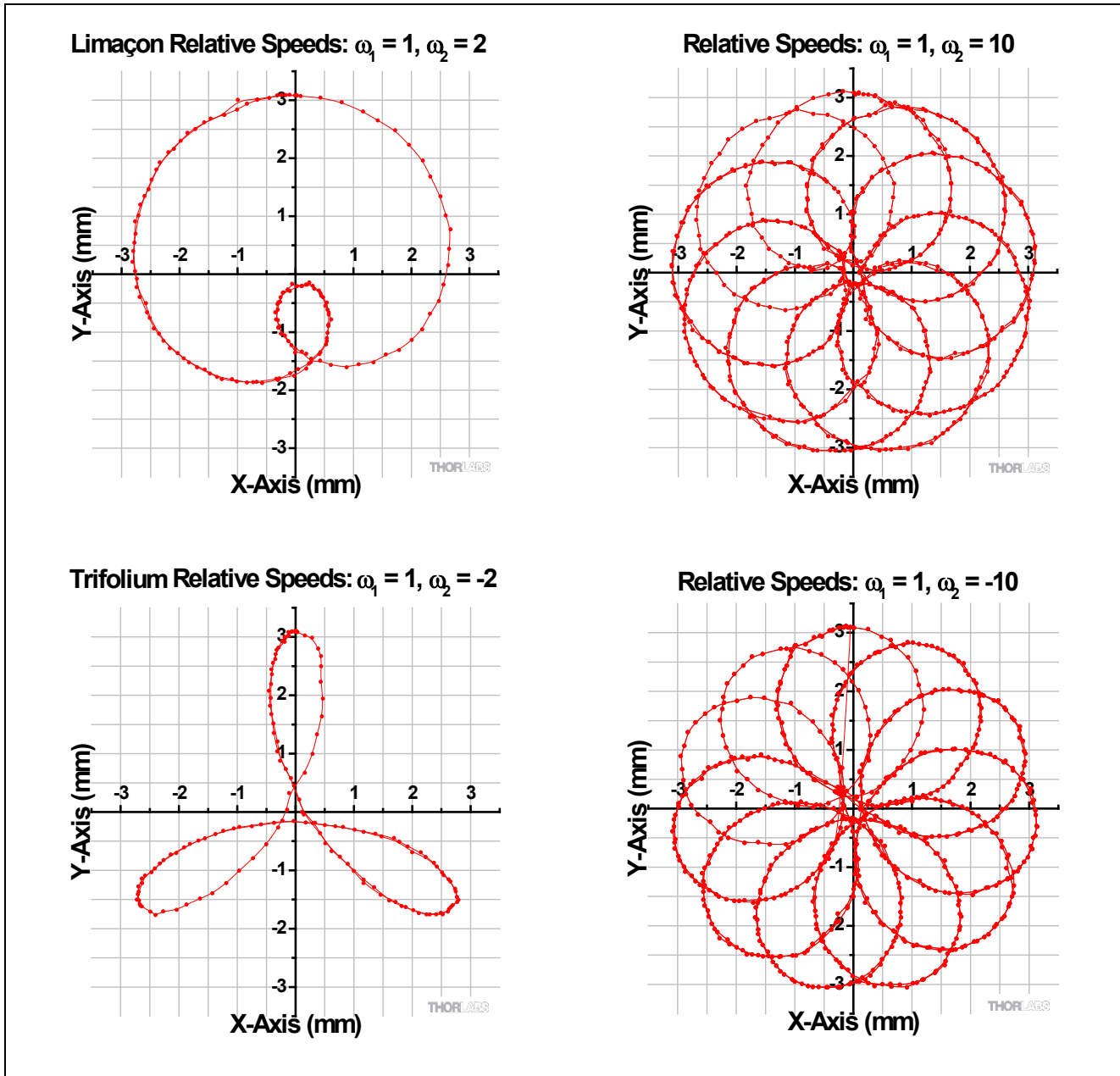


**Figure 10: Shown here are the scan patterns collected from the Risley Prism Scanner construction for this experiment, with the relative prism speeds listed in each graph title.**

## 5.4. *Discrete Beam Pointing*

By using Eq. (24), rasterized point scans were created. The patterns shown below were done with the dual wedge scanner. Figure 11 presents a 3.6 x 3.6 mm pattern that generated was by the LabVIEW itself. Step size was set as 1.2 mm, creating a field of 16 points. Our LabVIEW program was designed to scan the space from top to bottom, left to right. Figure 12 is a demonstration of how this scanner can be programmed to create any designed pattern, not just Rose Curves. This pattern will still be a non-continuous scan, as the prisms will need to reposition after each point measurement.
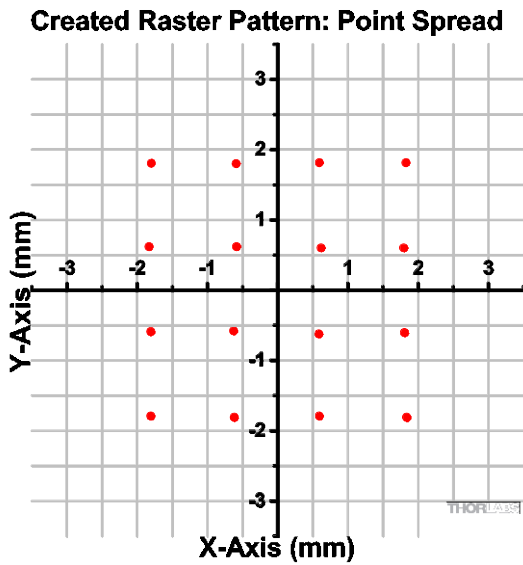
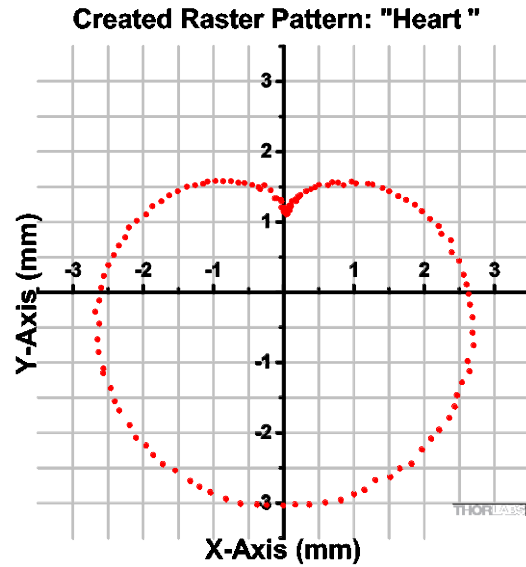**Figure 11: Point Spread Pattern Generated by Software**

**Figure 12: Uploaded Pattern in the Shape of Heart**

# Part 6. Summary

Dual wedge scanner can perform continuous scans and non-continuous raster scans. For continuous scans, the scan pattern is dictated by the rotation direction of each wedged prism and the ratio of rotation speeds between wedges. Non-continuous raster scans can be used to generate any pattern or scan a desired point.

Additionally, there are a few limitations for dual wedge scanners:

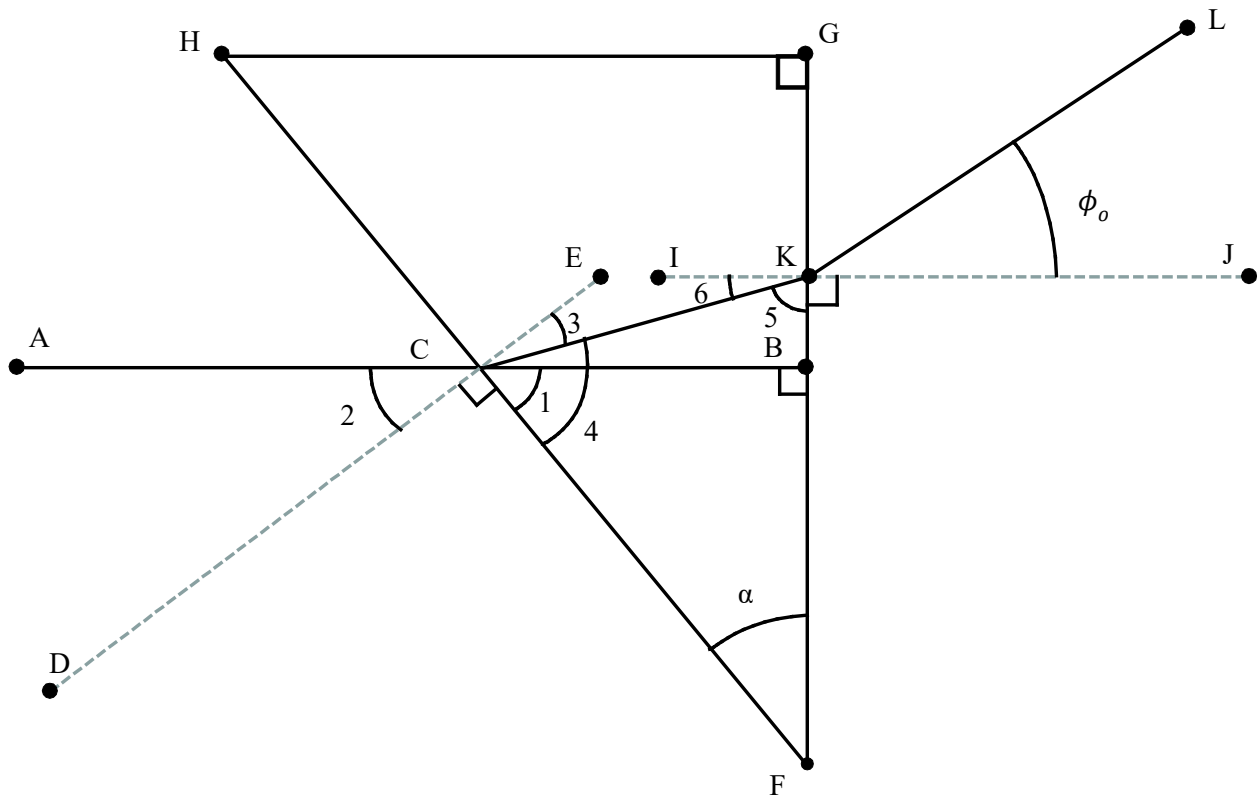1.  There is always a center defect, regardless of the type of scan being performed, that the beam can not be pointed in.

2.  Scanning area is dictated by wedge angle, prism thickness, and distance from the last optical surface to the scan surface.

3.  The system is very sensitive to misalignments, and must be constructed very well. Distortions in the scanning pattern can appear when misalignments of a few degrees are present.

## Part 7.  Appendix

### 7.1. Proof: Small Angle Equation Showing Beam Can Enter from Either Side of a Prism

Given the wedge angle and that the incoming beam is incident on the wedged side, perpendicular to the flat face, prove: $\phi_o = (n_g - 1)\alpha$. Assume that the refractive index of air is 1.

Below is a diagram of the interaction, where angles are labeled with numbers and points are labeled with letters.

Proof:

| Statements | Reasons |
|---|---|
| 1. $\overline{AB}$ is perpendicular to $\overline{FG}$ of $\varDelta FGH$<br>∠FGH = 90°<br>∠HFG = α | Given |
| 2. ∠1 + ∠α + 90° = 180° | $\varDelta CBF$ |
| 3. ∠1 + ∠2 + 90° = 180° | Supplementary Angles of $\overline{AB}$ |
| 4. ∠α = ∠2 | Solve 2. and 3. for ∠α |
| 5. Create $\angle 3 = \sin^{-1}\left(\dfrac{\sin(\alpha)}{n_g}\right)$ | Snell's Law Interaction |
| 6. ∠3 + ∠4 = 90° | Complementary Angles of ∠ECF |
| 7. $\angle 4 = 90 - \sin^{-1}\left(\dfrac{\sin(\alpha)}{n_g}\right)$ | Solve 6. for ∠4 substituting ∠3 from 5. |
| 8. ∠4 + ∠α + ∠5 = 180° | $\varDelta CFB$ |
| 9. $\angle 5 = 180 - \angle\alpha - 90° + \sin^{-1}\left(\dfrac{\sin(\alpha)}{n_{glass}}\right)$ | Solve 8. for ∠5 substituting ∠4 from 7. |
| 10. ∠5 + ∠6 = 90° | Complementary Angles of ∠IKF |
| 11. $\angle 6 = 90° - 180° + \angle\alpha + 90° - \sin^{-1}\left(\dfrac{\sin(\alpha)}{n_g}\right)$ | Solve 10. for ∠6 substituting ∠5 from 9. |
| 12. $\angle\phi_o = \sin^{-1}\left(n_g\sin(\angle 6)\right)$ is created | Snell's Law Interaction |
| 13. $\phi_o = \sin^{-1}\left\{n_g\sin\left[\alpha - \sin^{-1}\left(\dfrac{\sin(\alpha)}{n_g}\right)\right]\right\}$ | Solve 12. substituting ∠6 from 11. |

The exit angle, $\phi_o$ is now expressed using the small angle approximation as:

$$\phi_o = \sin^{-1}\left\{n_g sin\left[\alpha - \sin^{-1}\left(\frac{\sin(\alpha)}{n_g}\right)\right]\right\} \approx n_g\left(\alpha - \frac{\alpha}{n_g}\right) = (n_g - 1)\alpha$$

This is equivalent to what is shown in Part 2.

### 7.2. Proof: Two Prisms Cause Twice the Exit Angle of a Single Prism

Given two identical prisms sharing their flat sides, prove that the exit angle with respect to the optical axis is twice as large as the exit angle with respect to the optical axis of one prism.

Below is a diagram of the interaction, where angles are labeled with numbers and points are labeled with letters.
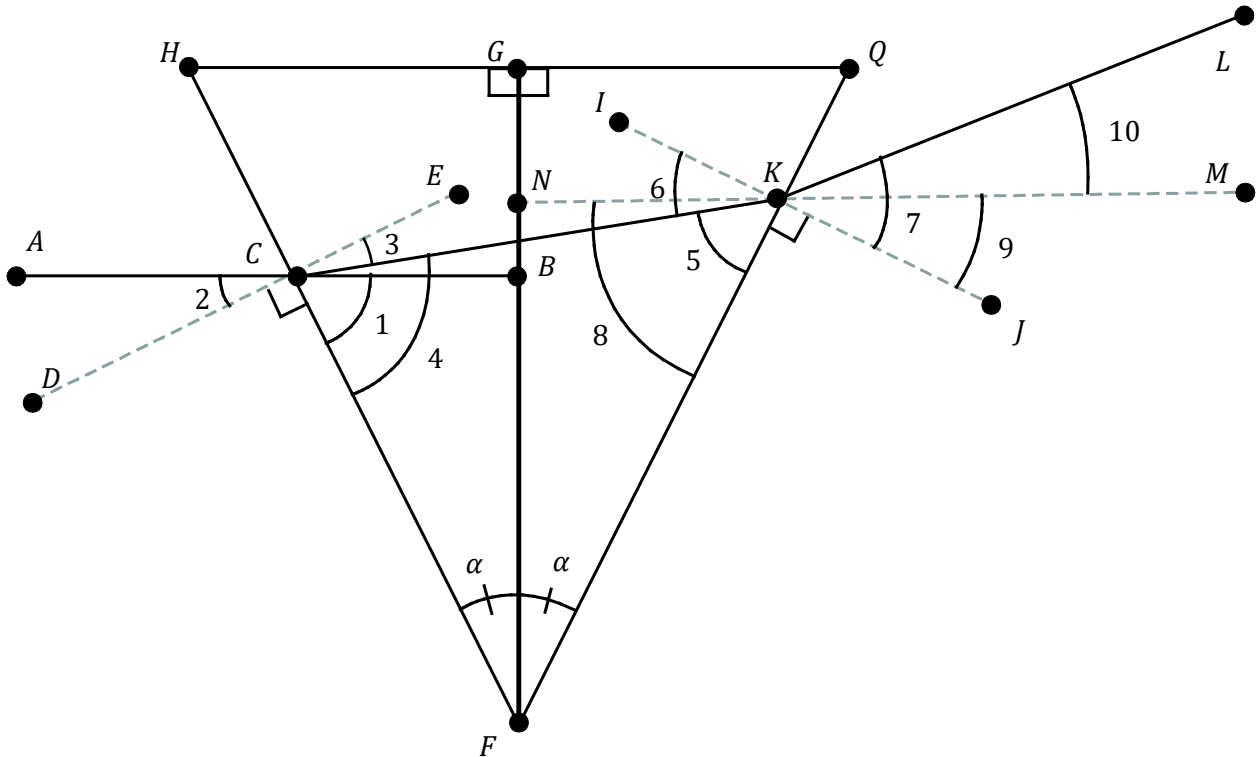
Proof:

| Statements | Reasons |
|---|---|
| 1. $\overline{AB}$ is perpendicular to $\overline{FG}$ of $\varDelta FGH$<br>$\varDelta FGH$ and $\varDelta FGQ$ are congruent<br>$\angle HFG = 90°$<br>$\angle HFG = \angle QFG = \alpha$ | Given |
| 2. $\angle 1 + \angle \alpha + 90° = 180°$ | $\varDelta CBF$ |
| 3. $\angle 1 + \angle 2 + 90° = 180°$ | Supplementary Angles of $\overline{AB}$ |
| 4. $\angle \alpha = \angle 2$ | Solve 2. and 3. for $\angle \alpha$ |
| 5. Create $\angle 3 = \sin^{-1}\left(\frac{\sin(\alpha)}{n_g}\right)$ | Snell's Law Interaction |
| 6. $\angle 3 + \angle 4 = 90$ | Complementary Angles of $\angle ECF$ |
| 7. $\angle 4 = 90 - \sin^{-1}\left(\frac{\sin(\alpha)}{n_g}\right)$ | Solve 6. for $\angle 4$ substituting $\angle 3$ from 5. |
| 8. $\angle 4 + 2*\angle \alpha + \angle 5 = 180$ | $\varDelta CFK$ |
| 9. $\angle 5 = 180 - 2*\angle \alpha - 90 + \sin^{-1}\left(\frac{\sin(\alpha)}{n_g}\right)$ | Solve 8. for $\angle 5$ substituting $\angle 4$ from 7. |
| 10. $\angle 5 + \angle 6 = 90$ | Complementary Angles of $\angle IKF$ |
| 11. $\angle 6 = 90 - 180 + 2*\angle \alpha + 90 - \sin^{-1}\left(\frac{\sin(\alpha)}{n_g}\right)$ | Solve 10. for $\angle 6$ substituting $\angle 5$ from 9. |
| 12. $\angle 7$ is created | Snell's Law Interaction:<br>$\angle 7 = \sin^{-1}\left(n_g \sin(\angle 6)\right)$ |
| 14. $\angle 7 = \sin^{-1}\left\{n_g \sin\left[2\alpha - \sin^{-1}\left(\frac{\sin(\alpha)}{n_g}\right)\right]\right\}$ | Solve 12. substituting $\angle 6$ from 11. |
| 13. $\overline{MN}$ parallel to $\overline{AB}$ through K | Construct |
| 14. $\angle 1 = \angle 8$ | $\varDelta CFB$ and $\varDelta NFK$ share two angles and are therefore similar |
| 15. $\angle 8 + 90 + \angle 9 = 180$ | Supplementary Angles of $\overline{MN}$ |
| 16. $\angle 1 + 90 + \angle 9 = 180$ | Substituting 14. into 15. |

| | |
|---|---|
| 17. $\angle 9 = \angle \alpha$ | Set 16. equal to 2. |
| 18. $\angle 10 = \angle 7 - \angle 9$ | A whole quantity equal to the sum of its parts. |
| 19. $\angle 10 = \sin^{-1}\left\{ n_g sin\left[2\alpha - \sin^{-1}\left(\frac{\sin(\alpha)}{n_g}\right)\right]\right\} - \alpha$ | Solve 18. substituting 17. and 14. |

The exit angle with respect to the optical axis can then be simplified with the small angle approximation:

$$\angle 10 = \sin^{-1}\left\{ n_g sin\left[2\alpha - \sin^{-1}\left(\frac{\sin(\alpha)}{n_g}\right)\right]\right\} - \alpha \ = n_g\left(2\alpha - \frac{\alpha}{n_g}\right) - \alpha$$

Rearranging this exit angle:

$$\angle 10 = n_g\left(2\alpha - \frac{\alpha}{n_g}\right) - \alpha$$

$$= \alpha(2n_g - 1) - \alpha$$

$$= 2\alpha n_g - 2\alpha$$

$$= 2(n_g - 1)\alpha$$

This is twice the angle shown in Eq. (5).

$$= 2\phi_o$$

## 7.3. Proof: Epitrochoid Equivalence

Epitrochoids [ep-i-**troh**-koids] are defined as the roulette traced by a point attached to a circle rolling along the outside circumference of a stationary circle. The general equation for an Epitrochoid is

$$x(t) = (a \pm b)\cos(t) + h * \cos\left(\frac{a \pm b}{b}t\right),$$

$$y(t) = (a \pm b)\sin(t) + h * \sin\left(\frac{a \pm b}{b}t\right). \tag{25}$$

In some cases, this equation can also form Hypotrochoids, which are similarly the roulette traced by a point attached to a circle rolling along the inside circumference of another circle. Epitrochoids are created for $(a + b)$ and Hypotrochoids are created for $(a - b)$.

Eqs. (22) and (25) are equivalent. This can be shown by creating a sketch of a general Epitrochoid, as seen in Figure 13. If Circle B has a radius $b$ and is rotating around Circle A defined by radius $a$ along its surface without slipping, we can define the radius to which Circle B is rotating about Circle A as $r_1 + r_d = a + b$. The length $h$, will be equivalent to $r_2$.
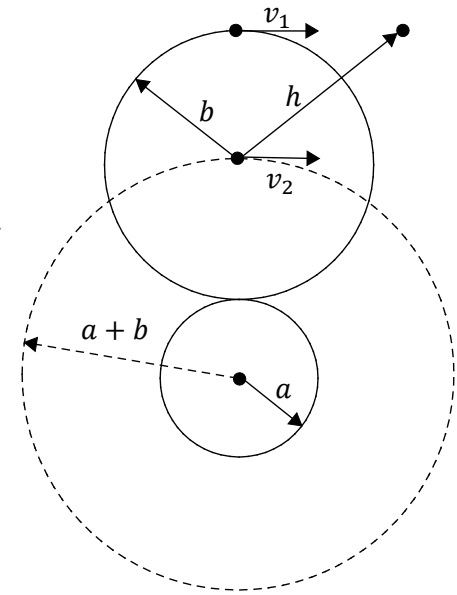
A point on Circle B is rotating with angular speed $\omega_1 = \frac{v_1}{b}$, while Circle B itself is rotating around Circle A with angular speed $\omega_2 = \frac{v_2}{a+b}$. Because Circle B does not slip while rotating along



**Figure 13: The diagram of an Epitrochoid.**

Circle A, $v_1 = v_2$, therefore, $\frac{\omega_1}{\omega_2} = \frac{a+b}{b}$. That is to say, the ratio of the angular speed of Circle B rotating about Circle A and the angular speed of Circle B rotating. Taking Eq. (22), made for two prisms spinning, and creating a ratio speeds by dividing each speed by $\omega_2$ shows that these and the general equation for Epitrochoids and Hypotrochoids, Eq. (25), are equivalent.

Rose Curves are a related class of shapes and have a general parametric form of:

$$x(\theta) = \cos(k\theta)\cos(\theta),$$

$$y(\theta) = \cos(k\theta)\sin(\theta) \tag{26}$$

Eq. (26) is equivalent to Eq. (22) by applying the Product-to-Sum Identities:

$$2\cos(\theta)\cos(\varphi) = \cos(\theta - \varphi) + \cos(\theta + \varphi),$$

$$2\sin(\theta)\sin(\varphi) = \sin(\theta - \varphi) + \sin(\theta + \varphi)$$

## 7.4. *Inherent Edge Distortion*

As shown in Part 3, the maximum exit angle of the Risley Prism Scanner is equivalent to the exit angle of a single prism, however, in Part 3.1 an approximation was applied:

$$r_r = r_1 + r_2 = z * \tan(2\phi_0) \approx 2z * \tan(\phi_o)$$

While this is true at small angles, it may cause a small amount of distortion near the edges, as this approximation essentially says that $r_1 = r_2$, which is not true. The values for these radii are:

$$r_1 = z * \tan(\phi_o)$$

$$r_2 = z * \tan(\phi_o) + \left\{ \left[ \frac{1}{2} (\cos(|\theta_1 - \theta_2|) + 1) \right] * [z * \tan(2\phi_o) - 2z * \tan(\phi_o)] \right\}$$

$r_2$ is shown to be equal to $r_1$ with a factor that accounts for the difference in height. The two radii will be equal when the prisms are 180° out of alignment, hence the term: $\left[ \frac{1}{2} (\cos(|\theta_1 - \theta_2|) + 1) \right]$. This will negate the factor when the prisms are out of phase, and add it back when $\theta_1 = \theta_2$.

## 7.5. Distortion Due to Home Position Misalignment

To demonstrate a rotation angle offset of the home prism locations, the following model was created using Eq. 24. The model shows the pointing locations of a raster scan assuming the use of two PS810-A wedge prisms, with no distance between the two prisms ($S = 0$), no tilt of the prisms with respect to the optical axis ($\beta = 0$), and a scanning surface 200 mm from the last surface of the second prism. Figure 14 shows the 0.5 mm step size raster scan within a 9 x 9 point pattern with zero offset ($\Delta\theta = 0$). It is important to note that the center point is off-center due to the center defect.
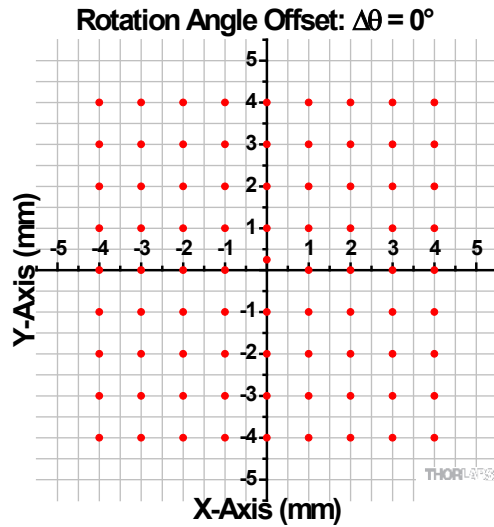


**Figure 14: Raster scan pattern if the Risley Prism scanner is properly aligned with a rotation angle offset $\Delta\theta = 0$.**

In Figure 15 and Figure 16 the rotation offset is Δθ = 5° and Δθ = -5°, respectively. Here it can be seen the positive offset resembles barrel distortion where the straight lines in Figure 14 and now curved away from the center of the field of view in Figure 15. In the case of the negative offset, the scan pattern resembles pincushion distortion, where the straight lines in Figure 14 and now curved in toward the center of the field of view if Figure 16.
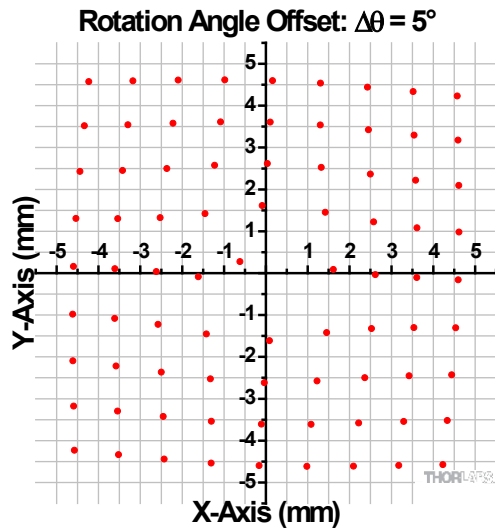


**Figure 15: The distorted raster scan created when there exists a rotation offset of 5° in the system.**
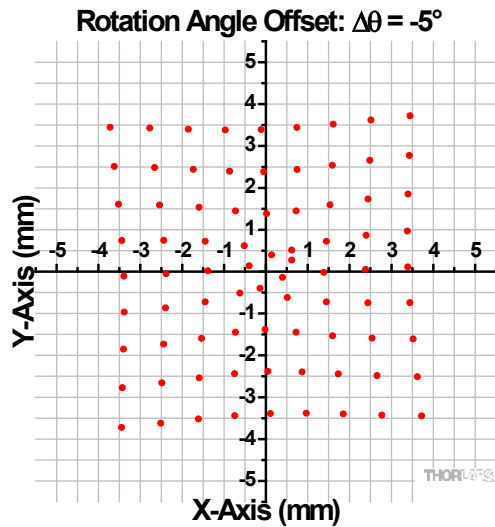


**Figure 16: The distorted raster scan created when there exists a rotation offset of -5° in the system.**

## 7.6. *Distortion Due to Prism Tilt*

Prism tilt can cause distortion in the image as well. To show this, consider point (4, 4) in Figure 14 at the edge of the scan. Assume there is no offset between wedges, but there is tilt between wedge and optical axis. Figure 17 present spot (4, 4) error when the $\beta_1$ changes from -10° to 10°, and $\beta_2$ set as 0°. Likewise for Figure 18, where the $\beta_2$ changes from -10° to 10° and $\beta_1$ is set to 0°



**Figure 17: This graph represents how the edge of an image created by a Risley Prism Scanner is distorted by Prism 1 being tilted between -10 and 10 degrees by showing the distance point (4, 4) from Figure 14 moves from its original position.**
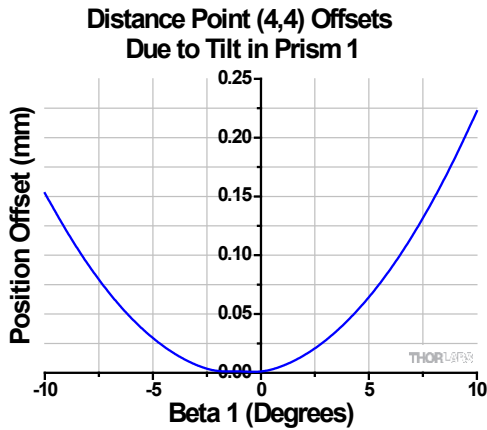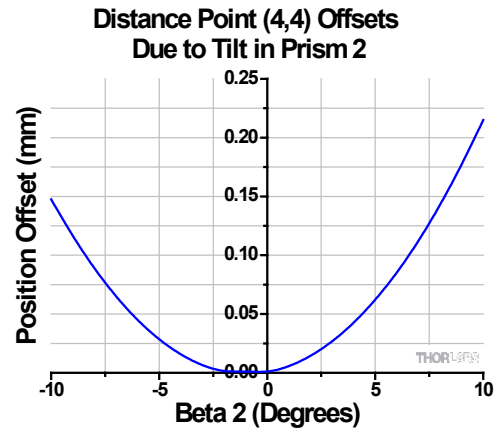
**Figure 18: This graph represents how the edge of an image created by a Risley Prism Scanner is distorted by Prism 2 being tilted between -10 and 10 degrees by showing the distance point (4, 4) from Figure 14 moves from its original position.**

## 7.7. Center Defect Variance Due to Tilt

Theoretically, the center defect's size wouldn't change when the distance between the scan surface and wedges, z, changes, but, in reality, assembly errors can make the center defect's size change according to the separation distance, $S$:

$$r_d = [2T + r_{total} * \tan(\alpha) * \cos(\Delta\theta)] * \tan(\phi_i - \phi_p) + S * \tan(\phi_0) + z * \tan(\gamma)$$

where $\gamma$ is the tilt angle between output laser beam and input laser beam. $\gamma$ is related to the wedge prism tilt angle by the following relation

$$\gamma = \alpha + \beta_2 - \sin^{-1}\left\{ n_g * \sin\left\{ \alpha - \sin^{-1}\left\{ \frac{\sin\left(\sin^{-1}\left(n_g * \sin\left(\alpha - \sin^{-1}\left(\frac{\sin(\alpha+\beta_1)}{n_g}\right)\right)\right) + \beta_1 + \beta_2\right)}{n_g}\right\}\right\}\right\},$$

which can be simplified with the small angle approximation to,

$$\gamma \approx 2\beta_2.$$

$\gamma$ is equal to twice the second wedge's tilt angle, if the tilt angle is very small.

There are two tilt conditions between the two wedges and center defect size change is differently depending on if $\gamma$ is positive or negative. When tilt of the second wedge is increased, $\gamma > 0$, center defect size will increase, as seen in Figure 19. When tilt of the second wedge is decreased, $\gamma < 0$, center defect size will first decrease to zero, then start increase, as seen in Figure 20.
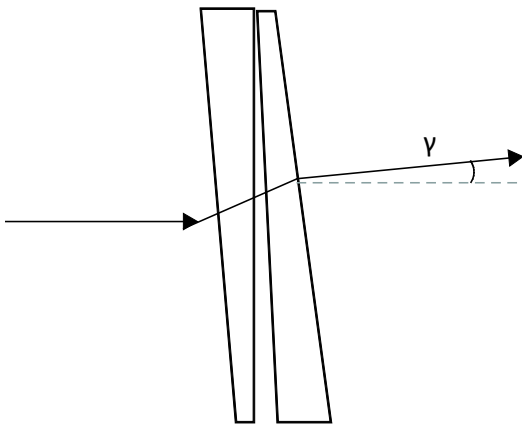


**Figure 19: A general case of when $\gamma > 0$, the center defect is expanded by the prism tilt.**
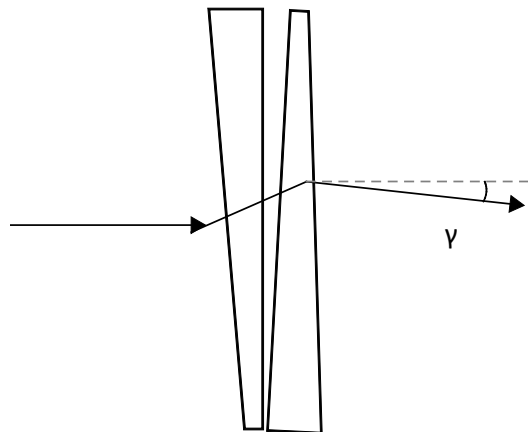
**Figure 20: A general case of when $\gamma < 0$, the center defect is reduced by the prism tilt then expand it again.**

## 7.8. Rose Curves by Speed Ratio

| | | Prism Speed 1 | | | | |
|---|---|---|---|---|---|---|
| | | 0 | 1 | 2 | 3 | 4 |
| Prism Speed 2 | 0 | | | | | |
| | 1 | | | | | |
| | 2 | | | | | |
| | 3 | | | | | |
| | 4 | | | | | |
| | 5 | | | | | |
| | 6 | | | | | |

|  |  | Prism Speed 1 | | | | |
|---|---|---|---|---|---|---|
|  |  | 0 | 1 | 2 | 3 | 4 |
| Prism Speed 2 | 0 |  | ○ | ○ | ○ | ○ |
|  | -1 | ○ | │ | ✿ | ✿ | ✿ |
|  | -2 | ○ | ✿ | │ | ✿ | ✿ |
|  | -3 | ○ | ✿ | ✿ | │ | ✿ |
|  | -4 | ○ | ✿ | ✿ | ✿ | │ |
|  | -5 | ○ | ✿ | ✿ | ✿ | ✿ |
|  | -6 | ○ | ✿ | ✿ | ✿ | ✿ |

## 7.9. *Derivation: Prism Angles as Functions of Scan Pattern Coordinates*

This derivation references both Figure 4 and Figure 5 and assumes the optical axis passes through the centers of two prisms, which can freely and independently rotate around the optical axis. The flat faces of the two prisms are adjacent, and there may or may not be a gap separating the prisms. The origin of this system is the point at which the optical axis intersects the wedged face of the first prism. The incident beam crosses the origin, and the scan pattern is located a distance $z$ from the wedged face of the second prism.

As discussed in Part 3, the two-dimensional scan pattern can be described as points $(x, y)$ on a plane orthogonal to the optical axis. The final form of these equations is provided in Part 4.1:

$$y(\theta_1, \theta_2) = (r_1 + r_d)\sin(\theta_1) + r_2 \sin(\theta_2 + \Delta\theta)$$
$$x(\theta_1, \theta_2) = (r_1 + r_d)\cos(\theta_1) + r_2 \cos(\theta_2 + \Delta\theta).$$

The angles $\theta_1$ and $\theta_2$, respectively, are the angular orientations of the first and second prisms, and the term $\Delta\theta$ accounts for angular misalignment. The term $r_d$ is the minimum possible radius of the center defect. The radii $r_1$ and $r_2$ are related to both $z$ and the thicknesses and wedge angles of the first and second prisms, respectively.

Alternate forms of these equations,

$$\theta_1(x, y) = \cos^{-1}\left(\frac{x^2 + y^2 + (r_1 + r_d)^2 - r_2{}^2}{2(r_1 + r_d)\sqrt{x^2 + y^2}}\right) + \tan^{-1}\left(\frac{y}{x}\right)$$
$$\theta_2(x, y) = \cos^{-1}\left(\frac{x^2 + y^2 - (r_1 + r_d)^2 + r_2{}^2}{2 r_2 \sqrt{x^2 + y^2}}\right) + \tan^{-1}\left(\frac{y}{x}\right) - \Delta\theta$$

are given in Part 4.3. The derivations of these two alternate equations follow.

**Derivation of $\theta_1(x, y)$**

Using substitutions $[A \equiv (r_1 + r_d)]$, $[B \equiv r_2]$, and $[\theta_3 \equiv \theta_2 + \Delta\theta]$ the starting equations become

$$y = A\sin(\theta_1) + B\sin(\theta_3)$$
$$x = A\cos(\theta_1) + B\cos(\theta_3).$$

The equations are arranged to separate the terms that include $\theta_3$ from the others,

$$y - A\sin(\theta_1) = B\sin(\theta_3)$$
$$x - A\cos(\theta_1) = B\cos(\theta_3)$$

and both equations are squared.

$$y^2 + A^2 \sin^2(\theta_1) - 2yA \sin(\theta_1) = B^2 \sin^2(\theta_3)$$
$$x^2 + A^2 \cos^2(\theta_1) - 2xA \cos(\theta_1) = B^2 \cos^2(\theta_3)$$

Adding these two equations together results in a relationship,

$$x^2 + y^2 + A^2(\sin^2(\theta_1) + \cos^2(\theta_1)) - 2A(y \sin(\theta_1) + x \cos(\theta_1)) = B^2(\sin^2(\theta_3) + \cos^2(\theta_3))$$

which provides an opportunity for the Pythagorean trigonometric identity $[\sin^2(\alpha) + \cos^2(\alpha) = 1]$ to simplify the third term on the left side, as well as eliminate terms dependent on $\theta_3$.

$$x^2 + y^2 + A^2 - 2A(y \sin(\theta_1) + x \cos(\theta_1)) = B^2$$

To isolate $\theta_1$, all but the trigonometric terms are moved to the right side of the equation,

$$x \cos(\theta_1) + y \sin(\theta_1) = \frac{x^2 + y^2 + A^2 - B^2}{2A}$$

and a trigonometric identity, whose derivation is shown below, is used to transform the left side of the equation into an equivalent expression.

$$\sqrt{x^2 + y^2} \cos\left(\theta_1 + \tan^{-1}\left(-\frac{y}{x}\right)\right) = \frac{x^2 + y^2 + A^2 - B^2}{2A}$$

The above expression becomes an equation for $\theta_1(x, y)$ by dividing both sides by the radical,

$$\cos\left(\theta_1 + \tan^{-1}\left(-\frac{y}{x}\right)\right) = \frac{x^2 + y^2 + A^2 - B^2}{2A\sqrt{x^2 + y^2}}$$

taking the inverse cosine of both sides,

$$\theta_1 + \tan^{-1}\left(-\frac{y}{x}\right) = \cos^{-1}\left(\frac{x^2 + y^2 + A^2 - B^2}{2A\sqrt{x^2 + y^2}}\right)$$

moving the inverse tangent term to the right side

$$\theta_1 = \cos^{-1}\left(\frac{x^2 + y^2 + A^2 - B^2}{2A\sqrt{x^2 + y^2}}\right) - \tan^{-1}\left(-\frac{y}{x}\right)$$

and replacing A and B with the specific variables.

$$\theta_1(x, y) = \cos^{-1}\left(\frac{x^2 + y^2 + (r_1 + r_d)^2 - r_2^2}{2(r_1 + r_d)\sqrt{x^2 + y^2}}\right) + \tan^{-1}\left(\frac{y}{x}\right)$$

**Derivation of $\theta_2(x, y)$**

The substitutions $[A \equiv (r_1 + r_d)]$, $[B \equiv r_2]$, and $[\theta_3 \equiv \theta_2 + \Delta\theta]$ are used again, but this time the terms including $\theta_1$ are moved to the right side.

$$y - B\sin(\theta_3) = A\sin(\theta_1)$$
$$x - B\cos(\theta_3) = A\cos(\theta_1)$$

Both equations are squared,

$$y^2 + B^2\sin^2(\theta_3) - 2yB\sin(\theta_3) = A^2\sin^2(\theta_1)$$
$$x^2 + B^2\cos^2(\theta_3) - 2xB\cos(\theta_3) = A^2\cos^2(\theta_1)$$

added together,

$$x^2 + y^2 + B^2(\sin^2(\theta_3) + \cos^2(\theta_3)) - 2B(x\cos(\theta_3) + y\sin(\theta_3)) = A^2(\sin^2(\theta_1) + \cos^2(\theta_1))$$

and simplified using the Pythagorean trigonometric identity $[\sin^2(\alpha) + \cos^2(\alpha) = 1]$. The result is an expression that does not include $\theta_1$.

$$x^2 + y^2 + B^2 - 2B(x\cos(\theta_3) + y\sin(\theta_3)) = A^2$$

These terms are then arranged so that those including $\theta_3$ are on the left,

$$x\cos(\theta_3) + y\sin(\theta_3) = \frac{x^2 + y^2 - A^2 + B^2}{2B}$$

and a trigonometric identity, which is derived below, provides an equivalent alternate expression for the terms on the left side.

$$\sqrt{x^2 + y^2}\cos\left(\theta_3 + \tan^{-1}\left(-\frac{y}{x}\right)\right) = \frac{x^2 + y^2 - A^2 + B^2}{2B}$$

The equation for $\theta_3(x, y)$ is then found by dividing both sides by the radical,

$$\cos\left(\theta_3 + \tan^{-1}\left(-\frac{y}{x}\right)\right) = \frac{x^2 + y^2 - A^2 + B^2}{2B\sqrt{x^2 + y^2}}$$

taking the inverse cosine of both sides,

$$\theta_3 + \tan^{-1}\left(-\frac{y}{x}\right) = \cos^{-1}\left(\frac{x^2 + y^2 - A^2 + B^2}{2B\sqrt{x^2 + y^2}}\right)$$

moving the inverse tangent term to the right side,

$$\theta_3 = \cos^{-1}\left(\frac{x^2 + y^2 - A^2 + B^2}{2B\sqrt{x^2 + y^2}}\right) - \tan^{-1}\left(-\frac{y}{x}\right)$$

and substituting in the correct values for A and B.

$$\theta_2 + \Delta\theta = \cos^{-1}\left(\frac{x^2 + y^2 - (r_1 + r_d)^2 + r_2^2}{2r_2\sqrt{x^2 + y^2}}\right) - \tan^{-1}\left(-\frac{y}{x}\right)$$

$$\theta_2(x,y) = \cos^{-1}\left(\frac{x^2 + y^2 - (r_1 + r_d)^2 + r_2^2}{2r_2\sqrt{x^2 + y^2}}\right) + \tan^{-1}\left(\frac{y}{x}\right) - \Delta\theta$$

**Equivalency of $[x\cos(\phi) + y\sin(\phi)]$ and $\left[\sqrt{x^2 + y^2}\cos\left(\phi + \tan^{-1}\left(-\frac{y}{x}\right)\right)\right]$**

Begin with the final form of the equation,

$$\sqrt{x^2 + y^2}\cos\left(\phi + \tan^{-1}\left(-\frac{y}{x}\right)\right).$$

The substitutions $\left[\rho = \sqrt{x^2 + y^2}\right]$ and $\left[\beta = \tan^{-1}\left(-\frac{y}{x}\right)\right]$ can be made to obtain the more familiar form,

$$\rho\cos(\phi + \beta),$$

which can be written in a different familiar form using an angle-sum trigonometric identity,

$$\rho\cos(\phi + \beta) = \rho\cos(\beta)\cos(\phi) - \rho\sin(\beta)\sin(\phi).$$

The right side of the equation is similar to $[x\cos(\phi) + y\sin(\phi)]$. If the two expressions are identical, $[x = \rho\cos(\beta)]$ and $[y = -\rho\sin(\beta)]$. The substitution for the inverse tangent term used at the beginning of this derivation can be used to investigate this question.

$$\beta = \tan^{-1}\left(-\frac{y}{x}\right)$$

This definition for $\beta$ is consistent with

$$x = \rho\cos(\beta)$$
$$y = -\rho\sin(\beta)$$

since the following is true.

$$\tan(\beta) = \frac{\rho\sin(\beta)}{\rho\cos(\beta)} = \frac{-y}{x}$$

In addition, the second substitution $\left[\rho = \sqrt{x^2 + y^2}\right]$, which is equivalent to $[\rho^2 = x^2 + y^2]$, can also be shown to be in agreement with the above proposed expressions for $x$ and $y$.

$$x^2 + y^2 = \rho^2 \cos^2(\beta) + \rho^2 \sin^2(\beta)$$

$$= \rho^2(\cos^2(\beta) + \sin^2(\beta))$$

$$= \rho^2$$

Therefore,

$$\sqrt{x^2 + y^2} \cos\left(\phi + \tan^{-1}\left(-\frac{y}{x}\right)\right) = x \cos(\phi) + y \sin(\phi).$$